

# Measurements of Jets containing Charm and Bottom Quarks with the ATLAS Detector

David Calvet<sup>1</sup> on behalf of the ATLAS Collaboration

<sup>1</sup>LPC Clermont-Ferrand, BP80026, 63171 Aubière cedex, France

DOI: <http://dx.doi.org/10.3204/DESY-PROC-2012-02/88>

The inclusive and dijet production cross-sections have been measured for jets containing  $b$ -hadrons ( $b$ -jets) in proton-proton collisions at the LHC using the ATLAS detector. The  $b$ -jets are identified using either a lifetime-based method or a muon-based method.  $D^{*\pm}$  meson production in jets is also measured, with fully reconstructed  $D^{*\pm}$  mesons. The results are compared to next-to-leading-order QCD predictions.

## 1 Introduction

Heavy flavour production in high-energy interactions provides an important test of perturbative QCD (pQCD). Calculations of the  $b$ -quark production cross-section have been performed at next-to-leading order (NLO) in pQCD and can be matched to different parton-shower and hadronisation models to produce final states that can be compared to those measured in collision data. Another method to study the production of heavy quarks is to measure  $D^{*\pm}$  mesons produced inside jets. With collisions at higher center-of-mass energy at the CERN Large Hadron Collider (LHC), the kinematical range accessible to experiment has been significantly extended. It is therefore of great interest to test the theoretical predictions at  $\sqrt{s} = 7$  TeV. This contribution reports a measurement of the inclusive  $b$ -jet and  $b\bar{b}$ -dijet production cross-sections, and a measurement of  $D^{*\pm}$  meson production in jets, both with the ATLAS detector [1].

## 2 Measurement of the inclusive and dijet cross-sections of $b$ -jets

The inclusive  $b$ -jet and  $b\bar{b}$ -dijet production cross-sections are measured using data recorded in 2010 with an integrated luminosity of  $34.0 \text{ pb}^{-1}$ . They are compared to next-to-leading order QCD predictions derived using POWHEG and MC@NLO [2]. To perform the parton-showering, POWHEG is interfaced to Pythia 6 and MC@NLO to Herwig 6 [2].

The relatively long lifetime of hadrons containing  $b$ -quarks is exploited to obtain a jet sample enriched in  $b$ -jets by selecting jets with a reconstructed secondary vertex significantly displaced from the primary vertex. The efficiency of the  $b$ -tagging is estimated with a data-driven method that uses jets containing a muon. The number of  $b$ -jets before and after  $b$ -tagging is obtained using the variable  $p_T^{\text{rel}}$ , which is defined as the momentum of the muon transverse to the combined muon plus jet axis. Muons originating from  $b$ -hadron decays having a harder  $p_T^{\text{rel}}$  spectrum than

muons in other jets, it is possible to obtain the fraction of  $b$ -jets in a given sample by fitting the  $p_T^{\text{rel}}$  spectrum using templates for  $b$ -,  $c$ - and light-flavour jets. Then, to estimate the number of  $b$ -jets in this enriched sample (the purity) a fit to the invariant mass distribution of the charged particle tracks in the secondary vertex is performed.

The  $p_T^{\text{rel}}$  method can also be used as a discriminant variable to measure the inclusive  $b$ -jet cross-section directly. The muon-based cross-section measurement relies on this method in the range  $30 < p_T < 140$  GeV and shows good agreement with the measurement obtained with the lifetime method.

The inclusive  $b$ -jet cross-section measurement as a function of jet  $p_T$  in the range  $20 < p_T < 400$  GeV and rapidity in the range  $|y| < 2.1$  is presented in Figure 1.

The normalized leading-order Pythia prediction shows broad agreement with the measured cross-section. As can be seen in Figure 2, the inclusive  $b$ -jet cross-section is found to be in good agreement with the POWHEG+Pythia prediction over the full kinematic range. MC@NLO+Herwig, however, predicts a significantly different behaviour of the double-differential cross section that is not observed in the data.

The  $b\bar{b}$ -dijet cross-section was measured as a function of dijet invariant mass in the range  $110 < m_{jj} < 760$  GeV, as a function of the azimuthal angle difference between the jets and of the angular variable  $\chi = \exp|y_1 - y_2|$  (see Ref. [1]). POWHEG+Pythia and MC@NLO+Herwig show good agreement with the measured  $b\bar{b}$ -dijet cross-sections, as does the normalized leading-order Pythia generator.

Both cross-section measurements are dominated by systematic uncertainties, mainly coming from the  $b$ -jet energy scale and the determination of the  $b$ -jet tagging efficiency and purity.

### 3 Measurement of $D^{*\pm}$ meson production in jets

The production of  $D^{*\pm}$  mesons inside jets is measured using data recorded between April and July 2010 with an integrated luminosity of  $0.30 \text{ pb}^{-1}$ .

Candidates for  $D^{*\pm}$  mesons inside jets are reconstructed in the decay chain:  $D^{*+} \rightarrow D^0 \pi^+$ ,  $D^0 \rightarrow K^- \pi^+$  and its charge conjugate. A  $D^0$  ( $\bar{D}^0$ ) candidate – combining two oppositely-charged tracks with  $p_T > 1$  GeV – whose mass is within 50 MeV of the PDG value is then combined with a third track with  $p_T > 0.5$  GeV having the same charge as the pion of the  $D^0$  ( $\bar{D}^0$ ) candidate. This  $D^{*\pm}$  candidate is required to have  $p_T > 7.5$  GeV, and the measured

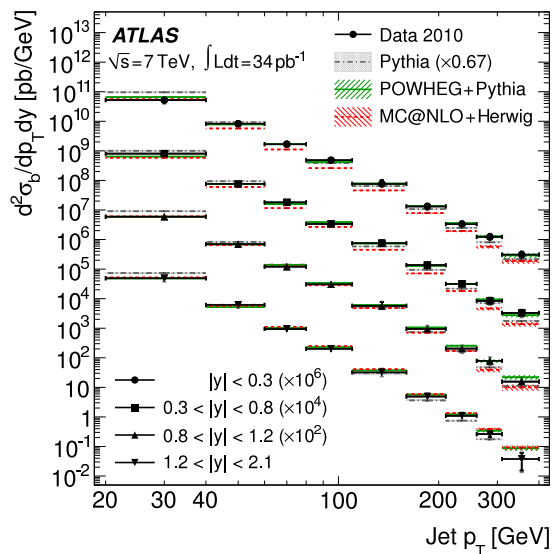


Figure 1: Inclusive double-differential  $b$ -jet cross-section as a function of  $p_T$  for different rapidity ranges [1]. The data are compared to the predictions of Pythia, POWHEG and MC@NLO.

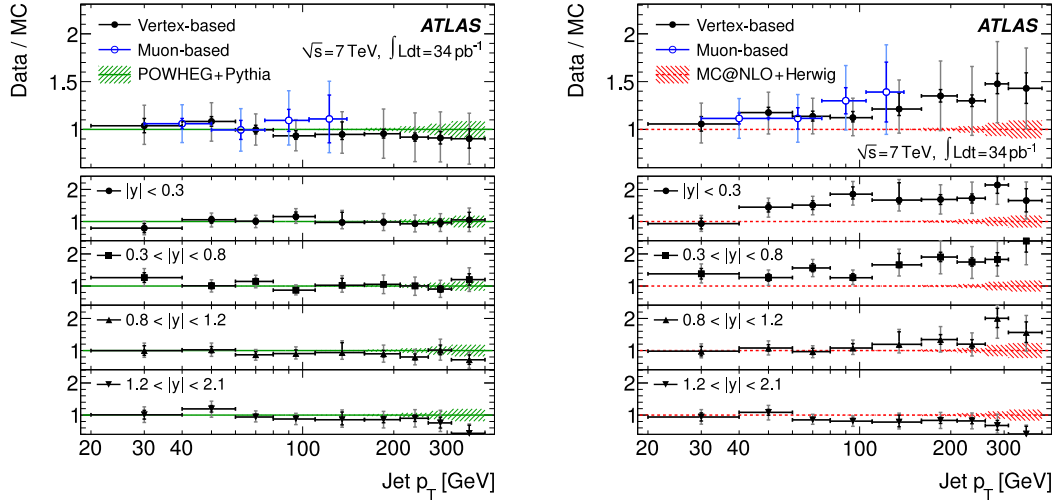


Figure 2: Ratio of the measured cross-sections to the theory predictions of POWHEG (left) and MC@NLO (right) [1]. In the region where the lifetime-based measurement overlaps with the muon  $p_T^{\text{rel}}$  measurement both results are shown. The top plot shows the full rapidity acceptance, while the four smaller plots show the comparison for each of the rapidity ranges separately. The data points show both the statistical uncertainty (dark colour) and the combination of the statistical and systematic uncertainties (light colour). The shaded regions around the theoretical predictions reflect the statistical uncertainty only.

$D^0$  ( $\bar{D}^0$ ) transverse decay length is required to be greater than zero. The reconstructed  $D^{*\pm}$  candidates are matched with the reconstructed jets in the event. The momentum fraction  $z = p_{||}(D^{*\pm})/E(\text{jet})$  of these candidates is required to be larger than 0.3. The  $D^{*\pm}$  jet yield is extracted from the distribution of the difference of the masses of the  $D^{*\pm}$  and  $D^0$  ( $\bar{D}^0$ ) candidates in bins of the jet  $p_T$  and  $z$ . After applying all the event selection and criteria, a total of  $4282 \pm 93$   $D^{*\pm}$  jet signal candidates are obtained. The distribution for the data integrated over all bins of  $p_T$  and  $z$ , together with the fit result, is shown in Figure 3.

The ratio  $\mathcal{R}(p_T, z) = N_{D^{*\pm}}(p_T, z)/N_{\text{jet}}(p_T)$  is calculated after a Bayesian iterative unfolding algorithm is applied to correct for the detector efficiency and bin-to-bin migration due to the detector resolution –  $N_{D^{*\pm}}$  is also corrected for the branching fraction  $\mathcal{B}(D^{*\pm} \rightarrow K^\mp \pi^\pm \pi^\pm)$ . The unfolding algorithm has been validated using Monte-Carlo (MC) simulated events and no bias is observed. The main systematic uncertainties come from trigger efficiency, track reconstruction efficiency and jet energy scale, see Ref. [1] for more details.

The measured  $D^{*\pm}$  jet production rate integrated over all the  $p_T$  and  $z$  bins is found to be  $\mathcal{R} = 0.025 \pm 0.001(\text{stat.}) \pm 0.004(\text{syst.})$  for  $D^{*\pm}$  jets with  $25 < p_T < 70$  GeV, in the range  $|\eta| < 2.5$  and with momentum fraction  $0.3 < z < 1$ . Measurements for different bins in  $p_T$  and  $z$  are available in Ref. [1]. Comparisons between the measurement and predictions from various MC calculations are shown in Figure 3 as a function  $z$ . The values of  $\mathcal{R}$  predicted by MC calculations are lower than the data by a factor 2 to 3 in the bins with lowest  $z$ , and this is especially significant at low  $p_T$ . The predictions are consistent with the data for  $z > 0.7$

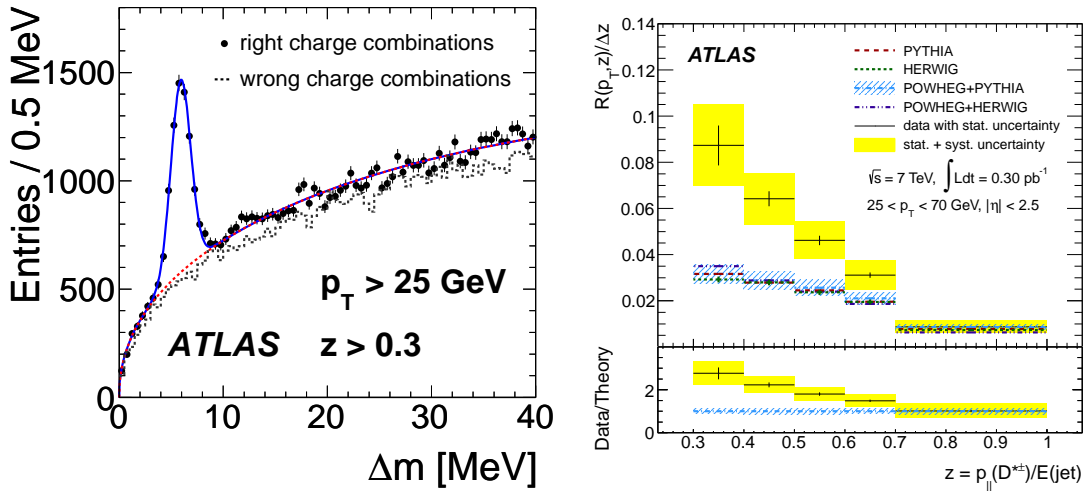


Figure 3: Left: distribution of the mass difference of the  $D^{*\pm} \rightarrow D^0\pi^+$  and its charge conjugate inside jets [1]. The solid line is the fit result. The dotted line represents the background component. Right: comparison of the  $D^{*\pm}$  production rate  $\mathcal{R}(p_T, z)/\Delta z$  in different  $z$  bins between the measurement and the MC predictions of Pythia, Herwig, POWHEG+Pythia and POWHEG+Herwig [1]. The inset shows the ratio of the measurement to the POWHEG+Pythia prediction.

at all  $p_T$ . Integrating over all the  $p_T$  and  $z$  bins, the production rate  $\mathcal{R}$  is estimated to be  $0.0133 \pm 0.0008$  by POWHEG+Pythia, which is just about half of the measured value.

## 4 Conclusions

The inclusive  $b$ -jet and  $b\bar{b}$ -dijet production cross-sections are found to be in good agreement with the POWHEG+Pythia predictions over the full kinematic range. MC@NLO+Herwig, however, predicts a significantly different behaviour for the inclusive  $b$ -jet double-differential cross section which is not present in the data. Nevertheless, it shows good agreement with the measured  $b\bar{b}$ -dijet cross-section.

In contrast, the measured production of  $D^{*\pm}$  mesons inside jets is not well modeled in any of the current MC generators. These results show the need of further QCD refinements to improve the description of high transverse momentum  $D$ -meson production in this new energy range of hadron collisions.

## References

- [1] ATLAS Collaboration, EPJ **C71** (2011) 1846; ATLAS Collaboration, Phys. Rev. **D85** (2012) 052005.
- [2] [Pythia] T. Sjöstrand, S. Mrenna, P. Z. Skands, JHEP **05** (2006) 026; [Herwig] G. Corcella *et al*, JHEP **01** (2001) 010; [POWHEG] P. Nason, JHEP **11** (2004) 040; S. Frixione, P. Nason, C. Oleari, JHEP **11** (2007) 070; S. Alioli, K. Hamilton, P. Nason, C. Oleari, E. Re, JHEP **04** (2011) 081; [MC@NLO] S. Frixione, B. R. Webber, JHEP **06** (2002) 029; S. Frixione, P. Nason, B. R. Webber, JHEP **08** (2003) 007